Carbohydrate Polymers 90 (2012) 210–217

Contents lists available at SciVerse ScienceDirect

Carbohydrate Polymers

journal homepage: www.elsevier.com/locate/carbpol

Bio-based nanocomposites obtained through covalent linkage between chitosan and cellulose nanocrystals

João P. de Mesquita, Claudio L. Donnici, Ivo F. Teixeira, Fabiano V. Pereira*

Departamento de Química, Universidade Federal de Minas Gerais, Av. Antônio Carlos, 6627 Pampulha, Belo Horizonte, MG, CEP 31270-901, Brazil

ARTICLE INFO

Article history:
Received 31 January 2012
Received in revised form 3 May 2012
Accepted 5 May 2012
Available online 12 May 2012

Keywords:
Chitosan
Cellulose nanocrystals
Bio-based nanocomposites

ABSTRACT

Bio-based nanocomposites were obtained through covalent linkage between cellulose nanocrystals (CNCs) and the natural polymer chitosan (CH). The CNCs were first functionalized with methyl adipoyl chloride (MAC) and the reactive end groups on the surface of the CNCs were reacted with the amino groups of the CH biopolymer in an aqueous medium. The functionalized CNCs and the resulting nanocomposites were characterized using FTIR, TEM, XRD, and elemental analyses. Characterization of the functionalized CNCs showed that up to 8% of the hydroxyl groups in the nanocrystals were substituted by the MAC residue. The covalent linkage between the CNCs and CH was confirmed by FTIR spectroscopy. The nanocomposites demonstrated a significant improvement in the mechanical performance and a considerable decrease in the hydrophilicity relative to the neat chitosan. The approach used in this work can be extended to other natural polymers.

1. Introduction

In the preparation of nanocomposites using different class of nanoparticles (such as nanoclays, carbon nanotubes or cellulose nanocrystals, CNCs), the most important property is the formation of a percolation network within the matrix.

In the case of composite materials prepared with polysaccharide nanocrystal such as CNCs or chitin nanocrystals (Muzzarelli, 2011), the achievement of an appropriate percolation network is a particular issue because the nanoparticles exhibit strong hydrogen bonding interactions between one another (Dufresne, 2010; Wang et al., 2012). These interactions can create large undesirable agglomerates within the polymer but, at the same time, the same interactions play an important role to develop the desirable filler network inside the matrix. Thus, to obtain an appropriate percolation of the CNCs in a nanocomposite, it is necessary to disperse the nanocrystals within a polymer matrix and to maximize the interfacial adhesion between the dispersed CNCs and the polymer, while still maintaining the filler/filler hydrogen bonding interactions (Dufresne, 2010).

Several strategies have been developed during the last few years to achieve the dispersion of the nanocrystals in different polymers, including the use of surfactants or using the chemical surface modification of the nanowhiskers (de Menezes, Siqueira, Curvelo, & Dufresne, 2009; Petersson, Kvien, & Oksman, 2007). However, the use of surfactants to coat the high specific area of the nanocrystals prohibits the use of this strategy (Samir, Alloin, & Dufresne, 2005). Additionally, previous results indicated that nanocomposites prepared from modified nanoparticles typically exhibited a significant decrease in the mechanical performance because the surface groups can insulate the nanoparticles, thus preventing the desirable filler/filler interactions (Capadona et al., 2007).

An alternative method to prepare nanocomposites with CNCs consists of a polymer chain surface modification of the nanoparticles (Dufresne, 2010; Habibi et al., 2008; Lin, Chen, Huang, Dufresne, & Chang, 2009; Morandi, Heath, & Thielemans, 2009). Generally speaking, two different strategies have been used to obtain grafted chains on the surface of the nanoparticles: the "grafting from" and the "grafting onto" methods (Dufresne, 2010). In the first strategy, the polymer chains are formed using an in situ surface-initiated polymerization from the immobilized initiators on the substrate (Habibi et al., 2008). The second method (grafting onto) consists of attaching a pre-synthesized polymer chain to the surface of the nanoparticle (Azzam, Heux, Putaux, & Jean, 2010; Dufresne, 2010). Using this strategy, Labet, Thielemans, and Dufresne (2007) prepared starch nanoparticles grafted with poly(tetrahydrofuran), poly(caprolactone), and poly(ethylene glycol) monobutyl ether chains using toluene 2,4-diisocyanate as the linking agent. More recently, Azzam et al. (2010) described the preparation of thermally responsive polymer-decorated cellulose-nanocrystals.

Abbreviations: CNC, cellulose nanocrystal; CH, chitosan; MAC, methyl adipoyl chloride.

* Corresponding author. Tel.: +55 31 3409 5753; fax: +55 31 3409 5700.
E-mail address: fabianovargas@yahoo.com (F.V. Pereira).

0144-8617/$ – see front matter © 2012 Elsevier Ltd. All rights reserved.
http://dx.doi.org/10.1016/j.carbpol.2012.05.025

Herein, we describe the preparation of a bio-based nanocomposite obtained through covalent linkage between cellulose nanowhiskers and a natural biopolymer, chitosan (CH). We have chosen CH because it is one of the strongest natural polymers and also because it contains reactive amino groups. Moreover, this biopolymer exhibits some important properties, such as biocompatibility, biodegradability and anti-bacterial properties, which make it a suitable material for biomedical applications, including drug delivery, tissue engineering, wound healing and various antimicrobial strategies (Dash, Chiellini, Ottenbrite, & Chiellini, 2011). In addition to biomedical applications, CH films have also been used for food packaging, mainly because of their non-toxicity and biodegradability (de Azeredo, 2009). However, the relatively weak mechanical properties of this biopolymer (in comparison to petroleum-based polymers) and its inherent water sensitivity restrict the wide use of chitosan films, particularly in environments where moisture is present (Sebti, Chollet, Degraeve, Noel, & Peyrol, 2007).

In this work the CNCs surface was functionalized, creating reactive end groups on the nanocrystals which reacted with the amino groups of the CH biopolymer, leading to a bionanocomposite with covalent linkage between the CNCs and the chitosan. The functionalized CNCs and the nanocomposites were characterized using different techniques, including FTIR, TEM, XRD, and elemental analyses.

2. Experimental

2.1. Materials

Highly deacetylated chitosan polymer was supplied by the Phytomare® Food Supplements. The degree of chitosan deacetylation (92%) was determined by potentiometric titration, Fourier transform infrared (FTIR) spectrometry and ^{1}H NMR. Eucalyptus wood pulp was kindly supplied by the Bahia Pulp Company (Brazil). Sulfuric acid and acetone were purchased from Synth. Methyl adipoyl chloride (MAC), triethylamine and toluene were purchased from Sigma–Aldrich.

2.2. Preparation of cellulose nanocrystals

A sulfuric acid hydrolysis reaction was performed with eucalyptus wood pulp according to a procedure described in the literature and in our previous work, with minor modifications (de Mesquita, Donnici, & Pereira, 2010; de Mesquita et al., 2011; de Rodriguez, Thielemans, & Dufresne, 2006). After a bleach treatment of the pulp, a controlled acid hydrolysis was performed by adding 10.0 g of cellulose to 160.0 mL of 64 wt% sulfuric acid under strong mechanical stirring. Hydrolysis was performed at 50 °C for approximately 40 min. After hydrolysis, the dispersion was washed with three cycles of centrifugation and the last wash was performed using dialysis against deionized water until the dispersion reached a pH of ~6. Afterward, the dispersions were ultrasonicated with a Cole Parmer Sonifier cell disruptor, equipped with a microtip for 5 min.

2.3. Preparation of the bionanocomposites

The preparation of the nanocomposites with covalent linkage between chitosan and cellulose nanocrystals (CH-c-CNCs) consisted of two steps.

Firstly, the CNCs were functionalized using the methyl adipoyl chloride (MAC) reagent and then, the functionalized CNCs were reacted with amino groups of the chitosan to produce bionanocomposites with different concentrations of nanocrystals. Typically, the chemical surface modification of the CNCs was performed in toluene at 60 °C for 4 h using constant mechanical stirring. The suspension of CNCs in toluene was obtained using a solvent exchange procedure (Siqueira, Bras, & Dufresne, 2009) where the original aqueous CNCs suspension was solvent exchanged with acetone followed by toluene, using three successive centrifugation and redispersion steps for each solvent. Two different functionalized CNC were prepared and are named according to the MAC/CNC ratio (wt%) used in each reaction: MA-CNC-1.9 (MAC/CNC = 1.9) and MA-CNC-0.8 (MAC/CNC = 0.8). For the MA-CNC-1.9, 200 μL of MAC and 300 μL of triethylamine were added in a suspension of nanowhiskers (~0.5%, m/v) containing 120 mg of cellulose whiskers. For the MA-CNC-0.8, 80 μL of MAC and 130 μL of triethylamine were also added in a suspension of nanowhisker (~0.5%, m/v) containing 120 mg of CNCs. Triethylamine was used to catalyze the reaction and also to complex the HCl formed during the reaction (Thielemans, Belgacem, & Dufresne, 2006). After the reaction, a suspension of functionalized CNCs in water was obtained using another solvent exchange procedure, from toluene to acetone, and finally to water, using the same procedure described previously. Then, the aqueous suspension of functionalized CNCs was freeze-dried.

Secondly, for the preparation of chitosan covalently bonded to the functionalized nanocrystals, a CH solution was prepared adding the biopolymer in acetic acid (3%, w/v), and then, an appropriate amount of MA-CNC-1.9 or MA-CNC-0.8 (0, 1.0, 5.0, 10, 20, 30, 40, 50 or 60%, w/w) was added. The reaction was performed in the aqueous medium at room temperature, and the suspensions were stirred for 24 h. The bionanocomposites were named CH-c-CNC-1.9 or CH-c-CNC-0.8 when the nanocomposites were prepared with MA-CNC-1.9 or MA-CNC-0.8, respectively. For comparative purposes, nanocomposites were also prepared using a simple mixture of unmodified CNCs with CH (detailed results obtained from these samples are not shown here). These samples were named CH/CNCs.

2.4. Characterization

Transmission electron microscopy (TEM) was performed on samples using a FEI Tecnai G2-Spirit with a 120-kV acceleration voltage. The CNCs suspensions were deposited from an aqueous dispersion on a carbon–Formvar-coated copper (300-mesh) TEM grids. The samples were subsequently stained with a 2% uranyl acetate solution to enhance the microscopic resolution.

Fourier transform infrared (FTIR) spectroscopy of the CNCs and the nanocomposites was recorded using a Nicolet 380 FTIR spectrometer (Nicolet, MN). The samples were prepared by using a KBr-disk.

Thermogravimetric analysis (TG/DTG) was performed using a DTG60 SHIMADZU. The samples were heated from room temperature to 600 °C using a heating ramp of 15 °C min^{-1} under N_2 flow (200 mL min^{-1}).

XRD measurements were performed on a SHIMADZU (XRD6000) X-ray diffractometer with a Cu Kα radiation source (λ = 0.154 nm) and in the 2θ range of 10–35° using a step intervals of 0.02°.

Elemental analysis was performed using a CHN Perkin-Elmer analyzer. The results obtained from this technique were used to determine the degree of substitution (DS), which is given by the number of hydroxyl groups substituted by MAC per unit of anhydroglucose. The methodology used here was recently reported by Siqueira, Bras, and Dufresne (2010). Using this methodology, the DS was calculated through the equation:

$$DS = \frac{72.07 - (C \times 162.14)}{(143.15 \times C) - 84.08}, \quad (1)$$

In this equation (Siqueira et al., 2010), C is the relative carbon content in the sample, and the numbers 72.07, 162.14, 143.15

and 84.08 are the relative carbon mass of the anhydroglucose unit ($C_6H_{10}O_5$), the molecular weight of the anhydroglucose, the molecular weight of the MAC residue linked to the anhydroglucose unit and the carbon mass of the MAC group, respectively. The experimental values were corrected by considering unmodified CNCs as pure cellulose, which correlates with a relative carbon content of 44.44%. Thus, the relative carbon content of the unmodified CNC was converted to this value (using the conversion factor = 1.113), and the same correction factor was applied to the functionalized CNCs. The obtained values were an average of two measurements.

Mechanical properties were obtained using a Lloyd testing instrument (model LS 500). Film strips of 6 cm × 1.5 cm (length × width) were cut from each preconditioned sample and mounted between the grips of the machine. The initial grip separation and crosshead speed were set to 50 mm and 12.5 mm/min, respectively. At least ten replicates of each specimen were averaged together.

The water uptake of the CH and the bionanocomposites was determined using the following procedure. The samples were cut into a 10 mm × 10 mm square and dried overnight at 90 °C. Next, the samples were submerged in distilled water for 48 h at room temperature until reach the equilibrium state. The degree of swelling of each sample was determined by the equation $W(\%) = (W_\infty - W_o)/W_o \times 100$, where W_∞ is the weight after 48 of submersion in distilled water (using a filter paper to remove the surface adsorbed water) and W_o is the initial dry weight of the sample. To compare the water absorption of the nanocomposites with the absorption of the neat chitosan, the $W(\%)$ values were converted into a relative degree of swelling, using the equation $W_r = W/W_{QT} \times 100$, where W_{QT} is the water absorption of the pure chitosan.

3. Results and discussion

3.1. CNCs functionalization

To prepare the CH-c-CNCs nanocomposites, the nanocrystals were first chemically modified using methyl adipoyl chloride (MAC) reagent. The selective functionalization of the CNCs was achieved via the reaction between the acyl chloride moieties of MAC and the hydroxyl groups of the nanocrystals, yielding functionalized CNCs with methyl ester end groups. MAC reagent has already been used in other selective syntheses (Moon et al., 2007; Regourd, Ali, & Thompson, 2007). The reaction route utilized to functionalize the CNCs is provided in Scheme 1.

It is important to mention here how the excess of unreacted MAC was discarded from the CNCs after the reaction. The functionalized CNCs, dispersed in toluene, were precipitated using centrifugation. The solid material was re-dispersed in toluene and then washed two more times with the same solvent. After that, the material was again washed with several cycles of centrifugation: three times with acetone and three times with water in order to completely discarded the excess of unreacted MAC reagent. This procedure was important to prove the covalent character between the MAC residue and the nanocrystals, ruling out possible adsorption of carboxylated MAC.

Thus, the functionalization of the nanocrystals was confirmed first by the FTIR technique (Fig. 1). The FTIR analysis of the freeze-dried nanocrystals suspensions revealed the appearance of an absorption band at 1725 cm^{-1}, characteristic of the C=O ester stretch band. This band was found for both types of functionalized CNCs, i.e., MA-CNC-1.9 and MA-CNC-0.8 (Fig. 1). In addition, the spectrum of the modified CNCs samples exhibited a narrower O—H stretching band (3360 cm^{-1}), due to a decrease in the amount of the hydrogen bonding between the nanoparticles. Moreover, the

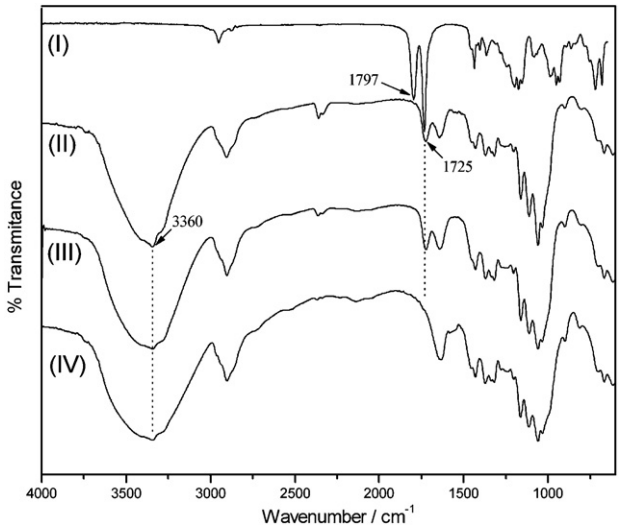

Fig. 1. FTIR spectra of the MAC reagent (I), MA-CNC-1.9 (II), MA-CNC-0.8 (III) and the unmodified CNC (IV).

signal at 1797 cm^{-1}, assigned to the acyl chloride function of the MAC reagent, was not observed in the spectra of the functionalized CNCs, indicating first a complete reaction between these groups with the hydroxyl groups of the CNCs and also a complete discard of the unreacted MAC reagent from the nanocrystals surface.

Fig. 2 shows a characteristic TEM image of the unmodified-CNC (a) and of the functionalized-CNC, MA-CNC-0.8 (b).

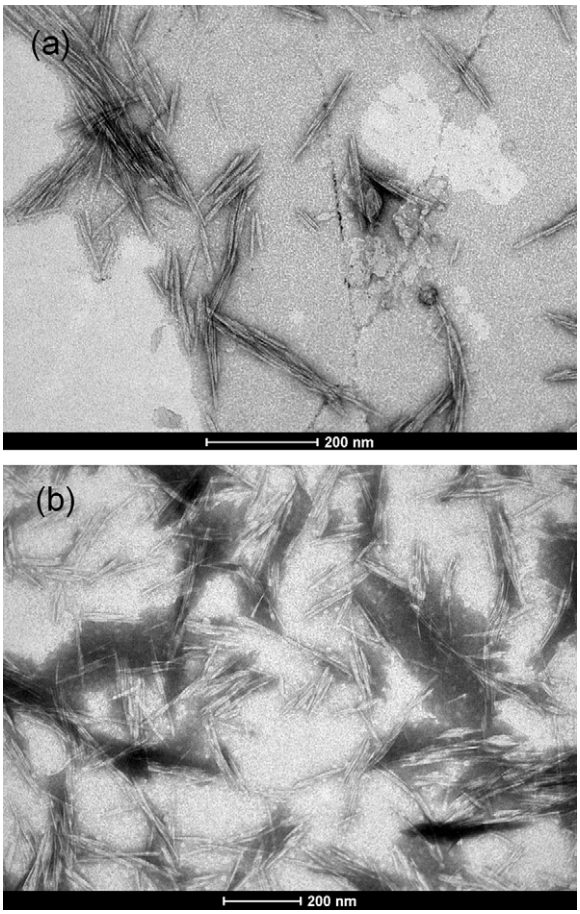

Fig. 2. TEM images of the unmodified-CNC (a) and functionalized-CNC, MA-CNC-0.8 (b).

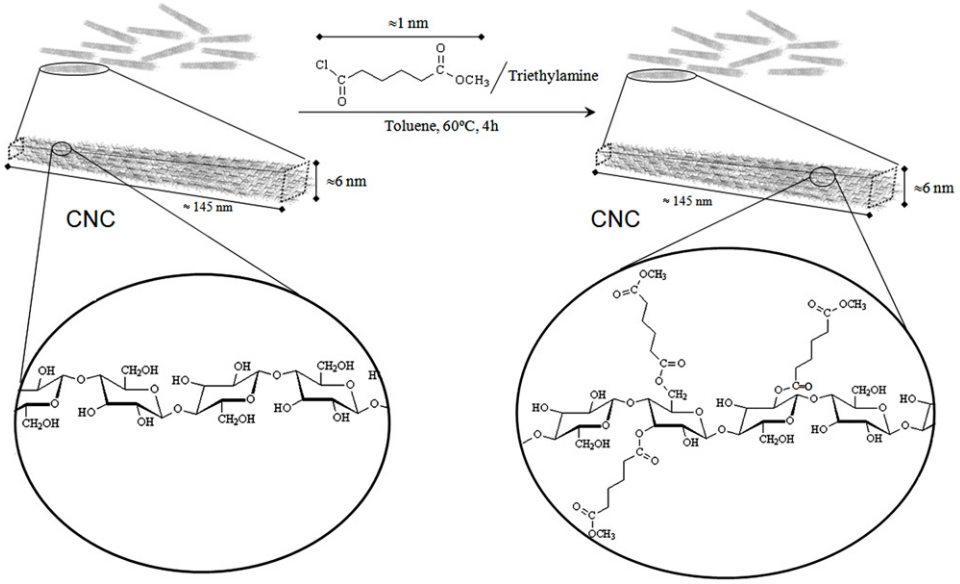

Scheme 1. Depiction of the reaction used to functionalize the CNCs with a methyl ester end group.

Using several TEM images, the mean values for the length (L) and diameter (D) of the unmodified rod-like nanocrystals were estimated to be 145 ± 25 nm and 6 ± 1.5 nm, respectively. Because the morphology of the nanocrystals plays a pivotal role in nanocomposite properties (Dufresne, 2010; Eichhorn, 2011), it is very important to ensure that the morphology of the CNCs was not significantly altered as a result of the chemical modification. The TEM results show that the morphology of the individual CNCs did not change after functionalization with the MAC reagent. The nanocrystals maintained their elongated morphology with the same length and aspect ratio as that of the unmodified CNCs. The TEM images obtained for the MA-CNC-1.9 were similar (not shown).

The analysis of the crystal structures of the modified nanowhiskers is another method to evaluate their structural integrity (Gousse, Chanzy, Excoffier, Soubeyrand, & Fleury, 2002; Habibi, Lucia, & Rojas, 2010). X-ray diffraction measurements were performed to determine whether the functionalization altered the crystallinity of the nanowhiskers. The unmodified CNCs and the functionalized CNCs (MA-CNC-0.8 and MA-CNC-1.9) exhibited the same X-ray diffraction pattern (supplementary data, Fig. S1). Three main peaks at 15°, 16° and 22.5° were observed for the three samples and are characteristic of the X-ray diffraction peaks for cellulose I. The crystallinity indexes of the different CNCs were estimated from the intensity ratio equation $(I_{002} - I_{AM})/I_{002} \times 100$ (Moran, Alvarez, Cyras, & Vazquez, 2008), where I_{002} is the intensity value of the peak at 2θ close to 23° (representing the crystalline material), and I_{AM} is the intensity value close to $2\theta = 18°$ (representing amorphous material in the CNCs). Although this method has often been used to calculate the crystallinity indexes, it has also been shown to underestimate the amorphous content (Park, Baker, Himmel, Parilla, & Johnson, 2010); therefore we only used it here for comparative purposes. The crystallinity indexes values obtained for the samples CNC, MA-CNC-0.8 and MA-CNC-1.9 were 84, 82 and 84%, respectively. These results, together with the TEM analysis, suggest that the functionalization did not alter the crystallinity or morphology of the nanoparticles and that the chemical modification took place only on the surface of the nanocrystals.

Because the hydroxyl groups are being replaced by the MAC residue, the functionalized nanostructures are expected to have a higher hydrophobic character than the unmodified nanocrystals. Fig. 3 shows the dispersions of the unmodified-CNC and MA-CNC-1.9 in water and in different organic solvents.

All of the dispersions were prepared using the same concentration ($c = 0.01\%$, m/v) and the photographs were taken 15 min after the preparation (with sonication) of the suspensions. The dispersability of the different samples show clear differences exist between the redispersion of modified-CNC and unmodified CNC that is related to a higher hydrophobic character of the MA-CNC-1.9 sample.

The unmodified CNCs were easily dispersed in water, whereas the MA-CNC-1.9 suspensions exhibited significant turbidity 15 min after the preparation of the dispersion in the aqueous medium. Comparing the dispersion obtained in moderately polar organic solvents, i.e., acetone ($\in = 20.7$), THF ($\in = 7.58$) and ethyl acetate ($\in = 6.0$), it can be observed that a complete phase separation and precipitation took place for the unmodified CNCs (Fig. 3a). On the other hand, in Fig. 3b, even though turbid dispersions were obtained in the same solvents, they did not present complete phase separation or precipitation as observed in Fig. 3a, showing an increase in the hydrophobic character of the functionalized CNCs. Similar results were obtained for the MA-CNC-0.8 functionalized cellulose nanocrystals.

Our main goal here is to use the functionalized nanoparticles as a precursor in the preparation of a CH-c-CNCs bionanocomposites. However, because the modified nanoparticles could be relatively dispersed in moderately polar organic solvents, the simple method proposed here for surface modification of the nanocrystals can also find use for the preparation of other nanocomposites with different hydrophobic polymers.

Elemental analysis of the functionalized CNCs was performed to confirm the successful grafting of the MAC residue on the surface of the nanoparticles and mainly to estimate the degree of functionalization. Table 1 shows the theoretical data (in parentheses) and the experimental data obtained from the elemental analysis. Considering a relative carbon content of 44.44% for the unmodified CNC (the theoretical value of the unmodified CNC as that of pure cellulose), the relative carbon content obtained experimentally for the samples was converted into a theoretical value. The conversion factor obtained ($f = 44.45/39.93$) was 1.113. This factor was then used to convert the experimental values into corrected values of %C for samples MA-CNC-0.8 and MA-CNC-1.9.

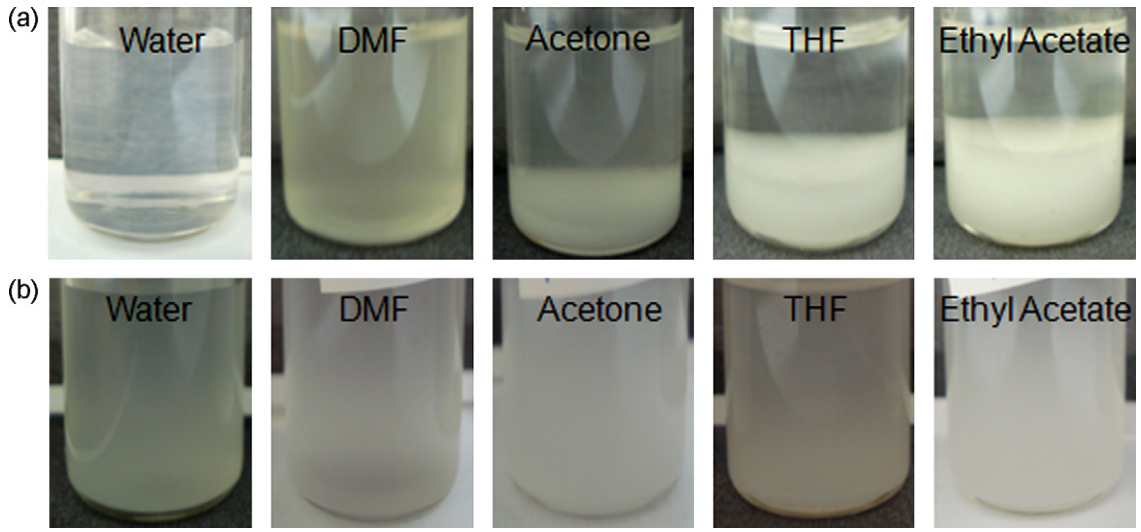

Fig. 3. Dispersibility of (a) unmodified-CNCs and (b) MA-CNC-1.9 in water and different organic solvents. All photographs were taken 15 min after the preparation of the suspensions (c = 0.01%, m/v) and sonication.

The DS values (calculated from Eq. (1)), were determined from the corrected values. After the functionalization of nanocrystals, the relative carbon content in the samples increased according to the amount of the MAC reagent used to modify the nanoparticles (Table 1). These values changed from 44.44% (unmodified CNCs) to 46.15% and 47.08%, for the MA-CNC-0.8 and MA-CNC-1.9 samples, respectively. The corresponding calculated DS values were 0.15 for the former and 0.25 for the latter. The interpretation of these data (Siqueira et al., 2010) is that the number of MAC residue grafted for each 100 anhydroglucose units was 15 for MA-CNC-0.8 and 25 for MA-CNC-1.9. By considering the amount of hydroxyl groups in each anhydroglucose unit, we calculated that ~5% and ~8% of the hydroxyl groups in the nanocrystals were substituted by the MAC residue for MA-CNC-0.8 and MA-CNC-1.9, respectively. The DS obtained in this work can be considered as relatively high because it is known that a low amount of grafted chains is generally sufficient to significantly modify the surface energy of cellulose (Buschlediller & Zeronian, 1992; Siqueira et al., 2010). Also, since the functionalization of the nanocrystals took place on the surface of the nanoparticles, the amount of surface hydroxyl groups substituted by the functionalized reagent is indeed significantly greater than 5% or 8%, changing the hydrophilic character of the nanoparticles, as shown in Fig. 3.

The thermal degradation behavior of the unmodified and functionalized CNCs was investigated using TGA measurements (Fig. S2). The functionalization and DS of the nanocrystals decreased the thermal stability of the nanoparticles at temperatures above 300 °C. This behavior can be explained by the decrease in the number of the hydrogen bonds in the modified nanoparticles (de Menezes et al., 2009), as the OH groups became substituted after the functionalization reaction.

Table 1
Elemental analysis data for the unmodified CNCs and functionalized CNCs with MAC reagent. The corrected elemental weight compositions are in parentheses.

Samples	%C	%H	%O	%N	DS
NCCs	39.93 (44.44)	5.43 (6.05)	54.14 (49.5)	0.50 (0)	–
MA-CNC-0.8	41.46 (46.15)	5.92 (6.59)	52.28 (47.26)	0.06 (0)	0.15
MA-CNC-1.9	42.28 (47.08)	5.49 (6.11)	52.14 (46.81)	0.09 (0)	0.25

3.2. Preparation of CH-c-CNCs bionanocomposites

To demonstrate that the functionalized-CNCs can react appropriately with a natural-based polymer in the expected manner, we combine the modified nanocrystals with chitosan biopolymer. The CH-c-CNCs bionanocomposites were prepared by the reaction of the functionalized nanocrystals (whose surface was decorated with methyl ester end-groups) with the reactive and nucleophilic amino groups of chitosan. The bionanocomposites films were prepared by solution casting immediately after the reaction. The reaction pathway is illustrated in Scheme 2.

After the preparation of the bionanocomposites, FTIR measurements were performed to verify the chemical bond formation between the functionalized CNCs and CH matrix. Although the selected reaction (Scheme 2) is highly expected to occur, the intrinsic difficulty of performing covalent linkages between the cellulose nanoparticles and the CH polymer chains should be considered. The main limitation in achieving a high density of covalent linkages is due to the steric hindrance and the potential of blocking of reactive sites by the grafted polymer chains (Morandi et al., 2009). Thus, a significant number of ungrafted CH chains are presumably found in the final nanocomposites.

Some studies described in the literature that have prepared nanocomposites through covalent linkages between the polymer and nanoparticles discussed the same intrinsic complexity that leads to a limited number of covalent linkages between the polymer and the nanoparticle. Typically, the final nanocomposites obtained are a mixture of the polymer chain-modified nanoparticles in a polymer matrix that forms a continuous interphase with improved interfacial adhesion (Chang, Ai, Chen, Dufresne, & Huang, 2009; Habibi et al., 2008; Yu, Ai, Dufresne, Gao, Huang, & Chang, 2008). We achieved a similar material as described in these works because the composites were prepared immediately after the reaction, without additional separation process or purification. Thus, the bionanocomposites are composed of a mixture of chitosan chain-modified nanoparticles in a chitosan matrix.

In order to probe the permanent linkage between the functionalized nanocrystals and CH, films of the bionanocomposites (prepared according to the procedure described in the experimental section) were sectioned and re-dispersed in acetic acid solution (5%, v/v). This dispersion remained under stirring for five days to remove the free chitosan that was not grafted on the surface of the CNCs. The CH-c-CNCs particles were then separated by

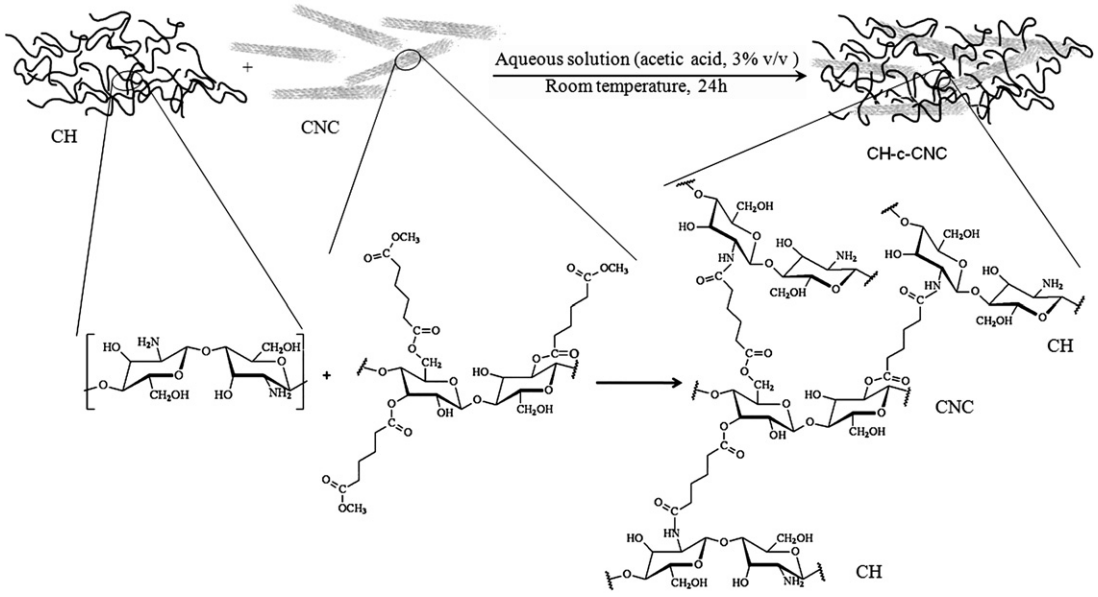

Scheme 2. Covalent linkage of chitosan on the surface of functionalized CNCs containing terminal ester groups.

centrifugation at 8000 rpm. The resulting precipitate was again dispersed in acetic acid solution for 24 h and centrifuged. This procedure was repeated 2 times to completely remove the ungrafted polymer (free chitosan) and the final product was dried using the acetone solvent. Fig. 4 shows the FTIR spectra obtained for the CH-c-CNC-1.9, separated according to the procedure described above. In order to compare, it is also showed in this figure the spectrum of the pure functionalized MA-CNC-1.9 nanocrystal and the spectrum of the neat chitosan. In the proposed reaction pathway (Scheme 2), the formation of amide groups is expected in the nanocomposite. However, the direct detection of the formation of the amide group through FTIR is rather difficult because the absorption band of this group overlaps with the peaks for the acetamide groups that are present in chitosan. Thus, for the purpose of comparison, we also conducted FTIR experiments with a composite prepared using the simple mixture of chitosan and the unmodified cellulose nanoparticles, CH/CNCs (Fig. S3). This sample was also prepared using the same acetic acid dispersion procedure, followed by centrifugation cycles to remove chitosan. We also provide the spectrum of the pure unmodified CNCs and neat CH in this figure.

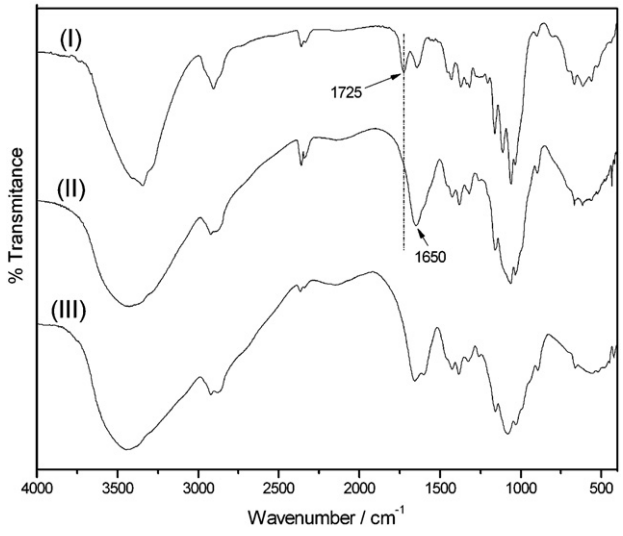

Fig. 4. FTIR spectrum of the functionalized MA-CNC-1.9 nanocrystal (I), CH-c-CNC-1.9 nanocomposite (II) and neat chitosan (III).

The MA-CNC-1.9 spectrum was compared with that of the nanocomposite CH-c-CNC-1.9 (Fig. 4). An important change observed after the grafting process was the disappearance of the C=O ester stretching vibration (at 1725 cm^{-1}). This result indicates the reaction of the ester end groups on the nanocrystals surface with the amino groups of chitosan. We also observed intensification of the band centered at 1650 cm^{-1}, which corresponds to the C=O stretching of the amide I group. Furthermore, the FTIR spectrum of the CH-c-CNC-1.9 nanocomposite exhibits remarkable differences from the spectrum obtained for the CH/CNCs mixtures. In the case of the composite CH/CNCs, no reaction took place and the entire contents of all of the chitosan was removed; thus, the spectrum of this composite (which is actually expected to be only the CNCs after the procedure used to remove CH from the unreacted composite) appears very similar to the one obtained from the pure and unmodified CNCs. These results indicate that the modified-cellulose nanofillers are covalently attached to the CH matrix.

It is important to mention that attempts to prepare films containing only CH-c-CNCs (after removing the ungrafted polymer) were not successful. Because there are many amino groups present throughout the chitosan matrix, the CH-c-CNCs obtained probably exist in a highly crosslinked system, preventing the dissolution of this material, which is necessary for processing the films using the casting technique.

To investigate the effect of the CNCs in the CH-c-CNC as reinforcing phase, we performed the classical tensile test. Fig. 5a shows stress–strain curves of the CH-c-CNC-0.8 films prepared with different concentrations of the nanocrystals. A remarkable increase in the tensile strength and modulus as a function of the concentration of the nanocrystals was observed. The strain-to-failure of the nanocomposites was similar to that of the pristine CH matrix when the concentration of CNCs was relatively low (up to approximately 10%). For higher concentrations of CNCs, a decrease in the strain-to-failure (from 12% to the pristine CH to 5% for the highest concentration used in this work) was observed. This behavior can be explained by the strong interfacial adhesion between the matrix and the cellulose nanofillers, which restricts the motion of the matrix.

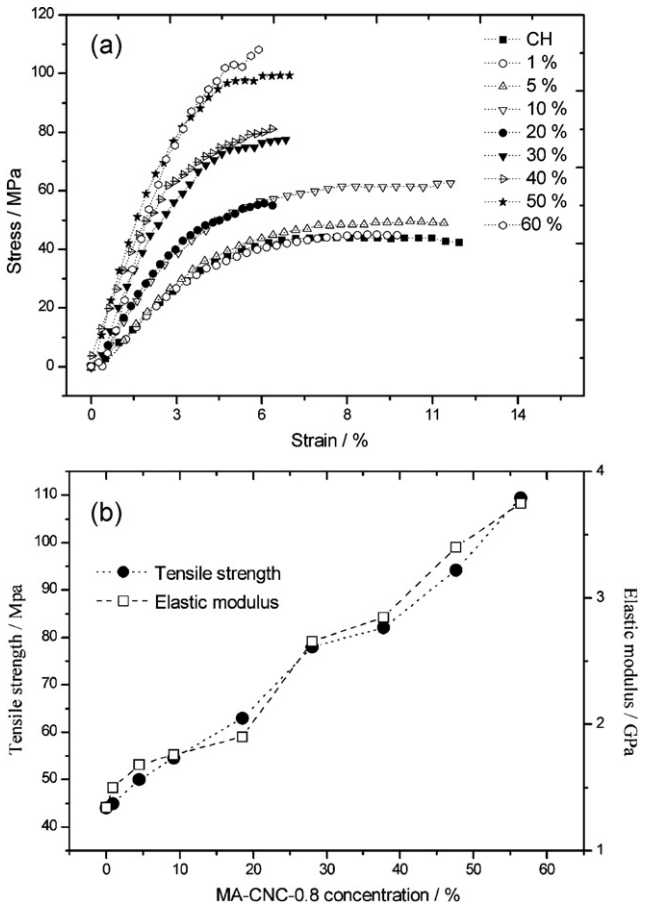

Fig. 5. (a) Stress–strain curves of pristine CH and chitosan-c-CNC-1.9 with different concentrations of CNCs and (b) tensile strength (•) and elastic modulus (□) as a function of the CNC-1.9 concentration. The dotted lines in (b) highlight the observed trends.

The modulus and the tensile strength (TS) were determined from the stress–strain curves, and the results are depicted in Fig. 5b, as a function of the CNCs concentration. A nearly linear increase in the TS and the modulus was observed with increasing nanowhiskers concentration. For the nanocomposite with the highest amount of nanocrystals (60%), an increase in the TS of approximately 150% relative to the pristine polymer was observed (from 45 MPa to 108 MPa), while the modulus increased up to 160% (from 1.2 GPa to 3.7 GPa).

For comparative purposes, we also carried out tensile tests with the nanocomposites CH-c-CNC-1.9 and with CH/CNC. Surprisingly, the mechanical properties were similar (not shown) to those obtained for the CH-c-CNC-0.8 (Fig. 5). These results are explained in the following manner. First, the CH is a very hydrophilic and polar matrix, and the nanowhiskers are sufficiently well dispersed in the polymer, even without covalent linkages between the nanofillers and the CH chains. Second, the strategy used here presents an intrinsic constraint regarding the limited number of covalent linkages between the nanoparticles and the polymer chains. Thus, the number of permanent linkages obtained between both species (CNCs and matrix) should not change considerably the spatial distribution of the nanoparticles within the matrix, resulting in a nanocomposite with similar mechanical properties compared to that observed for a mixture of unmodified CNCs and CH matrix (CH/CNCs composite).

However, a substantial difference in the water absorption behavior was observed when comparing the CH-c-CNC with the CH/CNC nanocomposites. CH is insoluble in pure water but

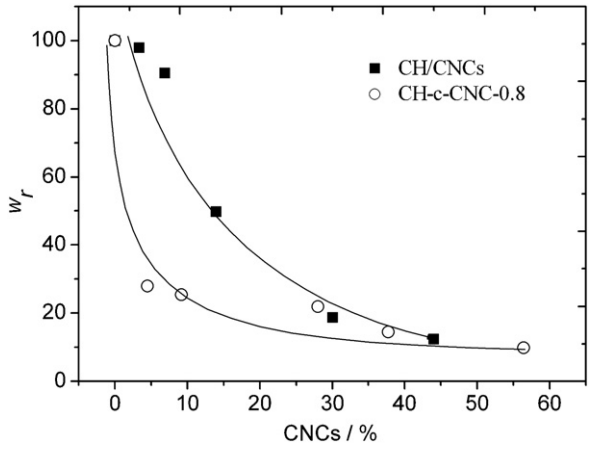

Fig. 6. Water uptake results for CH/CNCs and for CH-c-CNC-0.8 nanocomposites, as a function of CNC concentration.

can easily swell in this medium, which considerably decreases the mechanical properties and prevents its application and thus restricts its use in moist environments (Sebti et al., 2007). It has also been shown that chemical crosslinking inside a hydrophilic polymer matrix inhibits solubility or water absorption (Welsh & Price, 2003; Welsh, Schauer, Qadri, & Price, 2002). In addition, CNCs can effectively decrease the accessibility of water in hydrophilic matrixes. Previous results demonstrated that for starch/CNCs nanocomposites and also for chitosan/CNCs systems, the cellulose nanocrystals decreased the hydrophilicity of these matrixes, leading to a decrease in swelling (Cao, Chen, Chang, Stumborg, & Huneault, 2008; de Rodriguez et al., 2006; Li, Zhou, & Zhang, 2009). In a more recent study (de Paula, Mano, & Pereira, 2011), we demonstrated that a small amount of CNCs can be used to control the hydrolytic degradation of a polylactide polymer. This behavior was explained in terms of the high degree of crystallinity found in the nanocrystals which creates a tortuous path for the permeation of water and retards the hydrolytic degradation of the bionanocomposites.

We evaluate here not only the effect of the addition of CNCs in a hydrophilic matrix but also (and simultaneously), the effect of the covalent linkage between the matrix and the nanocrystals in the water uptake. Water uptake measurements were carried out using CH-c-CNC-0.8 and also with CH/CNCs. Both results are provided in Fig. 6. The water uptake for both nanocomposites decreased remarkably with increasing CNC concentration. However, this effect was considerably more pronounced for the CH-c-CNCs, mainly using low concentrations of nanofillers. At low concentrations of CNCs in the system CH-c-CNCs (approximately 10 wt%), the water swelling decreased to approximately 25% of the absorption observed for the neat chitosan, while for the mixed system CH/CNCs, the water swelling only decreased to approximately 90% of the value observed for pure chitosan.

As discussed by de Rodriguez et al. (2006), the three-dimensional network formed by hydrogen bonds between CNCs significantly inhibit the swelling and solubility of the nanocomposites in water.

In both nanocomposites compared in Fig. 6, a three-dimensional network formed by hydrogen bonds between CNCs is expected to occur. In addition, the decrease in the hydrophilicity of the nanocomposite CH-c-CNCs compared to CH-CNCs can be explained not only by the chemical functionalization of the nanocrystals, which increased the hydrophobic character of the nanoparticles, but also by the extra network formed by linkages between the CH matrix and the CNCs. Despite the limited number of such linkages, we believe this network can also plays a role and effectively inhibit

more water diffusion between the chains compared to a composite without the presence of those linkages.

The results for water uptake measurements using the MA-CNC-1.9 are similar to the nanocomposite obtained using MA-CNC-0.8 because, as explained in the mechanical properties results, the number of linkages is limited (for both, MA-CNC-1.9 and MA-CNC-0.8), by the steric hindrance and the potential of blocking of reactive sites by the grafted polymer chains.

4. Conclusion

Bio-based nanocomposites were obtained through covalent linkage between chitosan and functionalized cellulose nanocrystals. Characterization of the functionalization of the nanocrystals showed that the fraction of substituted hydroxyl groups was ~5% and ~8%, for MA-CNC-0.8 and MA-CNC-1.9, respectively. FTIR spectroscopy showed that the chitosan was covalently bonded onto the surface of the functionalized CNCs. The chitosan-c-CNCs nanocomposites demonstrated a significant improvement in mechanical performance (increase in tensile strength of up to 150%) compared to the neat chitosan. The results for water uptake measurements showed a remarkable decrease in hydrophylicity of chitosan, being this effect more pronounced for the CH-c-CNC nanocomposite compared to the system CH/CNCs. The approach used here can be extended to other natural polymers, such as collagen, to produce different bio-based nanocomposites with new properties and possible applications.

Acknowledgments

Authors thank CAPES (Nanobiotec – EDT N° 04/2008) and Pró-reitoria de Pesquisa – UFMG for the financial support. J.P. d. M. thanks the CNPq for funding a scholarship. The Centro de Microscopia-UFMG is also acknowledged for obtaining the TEM and SEM images.

Appendix A. Supplementary data

Supplementary data associated with this article can be found, in the online version, at http://dx.doi.org/10.1016/j.carbpol.2012.05.025.

References

Azzam, F., Heux, L., Putaux, J.-L., & Jean, B. (2010). Preparation by grafting onto, characterization, and properties of thermally responsive polymer-decorated cellulose nanocrystals. *Biomacromolecules*, *11*, 3652–3659.

Buschlediller, G., & Zeronian, S. H. (1992). Enhancing the reactivity and strength of cotton fibers. *Journal of Applied Polymer Science*, *45*, 967–979.

Cao, X., Chen, Y., Chang, P. R., Stumborg, M., & Huneault, M. A. (2008). Green composites reinforced with hemp nanocrystals in plasticized starch. *Journal of Applied Polymer Science*, *109*, 3804–3810.

Capadona, J. R., Van Den Berg, O., Capadona, L. A., Schroeter, M., Rowan, S. J., Tyler, D. J., et al. (2007). A versatile approach for the processing of polymer nanocomposites with self-assembled nanofibre templates. *Nature Nanotechnology*, *2*, 765–769.

Chang, P. R., Ai, F., Chen, Y., Dufresne, A., & Huang, J. (2009). Effects of starch nanocrystal-graft-polycaprolactone on mechanical properties of waterborne polyurethane-based nanocomposites. *Journal of Applied Polymer Science*, *111*, 619–627.

Dash, M., Chiellini, F., Ottenbrite, R. M., & Chiellini, E. (2011). Chitosan-A versatile semi-synthetic polymer in biomedical applications. *Progress in Polymer Science*, *36*, 981–1014.

de Azeredo, H. M. C. (2009). Nanocomposites for food packaging applications. *Food Research International*, *42*, 1240–1253.

de Menezes, A. J., Siqueira, G., Curvelo, A. A. S., & Dufresne, A. (2009). Extrusion and characterization of functionalized cellulose whiskers reinforced polyethylene nanocomposites. *Polymer*, *50*, 4552–4563.

de Mesquita, J., Donnici, C., & Pereira, F. (2010). Biobased nanocomposites from layer-by-layer assembly of cellulose nanowhiskers with chitosan. *Biomacromolecules*, *11*, 473–480.

de Mesquita, J., Patricio, P., Donnici, C., Petri, D., de Oliveira, L., & Pereira, F. (2011). Hybrid layer-by-layer assembly based on animal and vegetable structural materials: Multilayered films of collagen and cellulose nanowhiskers. *Soft Matter*, *7*, 4405–4413.

de Paula, E. L., Mano, V., & Pereira, F. V. (2011). Influence of cellulose nanowhiskers on the hydrolytic degradation behavior of poly(D,L-lactide). *Polymer Degradation and Stability*, *96*, 1631–1638.

de Rodriguez, N. L. G., Thielemans, W., & Dufresne, A. (2006). Sisal cellulose whiskers reinforced polyvinyl acetate nanocomposites. *Cellulose*, *13*, 261–270.

Dufresne, A. (2010). Processing of polymer nanocomposites reinforced with polysaccharide nanocrystal. *Molecules*, *15*, 4111–4128.

Eichhorn, S. J. (2011). Cellulose nanowhiskers: Promising materials for advanced applications. *Soft Matter*, *7*, 303–315.

Gousse, C., Chanzy, H., Excoffier, G., Soubeyrand, L., & Fleury, E. (2002). Stable suspensions of partially silylated cellulose whiskers dispersed in organic solvents. *Polymer*, *43*, 2645–2651.

Habibi, Y., Goffin, A.-L., Schiltz, N., Duquesne, E., Dubois, P., & Dufresne, A. (2008). Bionanocomposites based on poly(epsilon-caprolactone)-grafted cellulose nanocrystals by ring-opening polymerization. *Journal of Materials Chemistry*, *18*, 5002–5010.

Habibi, Y., Lucia, L. A., & Rojas, O. J. (2010). Cellulose nanocrystals: Chemistry, self-assembly, and applications. *Chemical Reviews*, *110*, 3479–3500.

Labet, M., Thielemans, W., & Dufresne, A. (2007). Polymer grafting onto starch nanocrystals. *Biomacromolecules*, *8*, 2916–2927.

Li, Q., Zhou, J., & Zhang, L. (2009). Structure and properties of the nanocomposite films of chitosan reinforced with cellulose whiskers. *Journal of Polymer Science Part B-Polymer Physics*, *47*, 1069–1077.

Lin, N., Chen, G., Huang, J., Dufresne, A., & Chang, P. R. (2009). Effects of polymer-grafted natural nanocrystals on the structure and mechanical properties of poly(lactic acid): A case of cellulose whisker-graft-polycaprolactone. *Journal of Applied Polymer Science*, *113*, 3417–3425.

Moon, B. S., Park, M.-T., Park, J. H., Kim, S. W., Lee, K. C., An, G. I., et al. (2007). Synthesis of novel phytosphingosine derivatives and their preliminary biological evaluation for enhancing radiation therapy. *Bioorganic and Medicinal Chemistry Letters*, *17*, 6643–6646.

Moran, J. I., Alvarez, V. A., Cyras, V. P., & Vazquez, A. (2008). Extraction of cellulose and preparation of nanocellulose from sisal fibers. *Cellulose*, *15*, 149–159.

Morandi, G., Heath, L., & Thielemans, W. (2009). Cellulose nanocrystals grafted with polystyrene chains through surface-initiated atom transfer radical polymerization (SI-ATRP). *Langmuir*, *25*, 8280–8286.

Muzzarelli, R. A. A. (2011). Chitin nanostructures in living organisms. In N. S. Gupta (Ed.), *Chitin: Formation and diagnosis*. Dordrecht: Springer Netherlands, pp. 1–34

Park, S., Baker, J. O., Himmel, M. E., Parilla, P. A., & Johnson, D. K. (2010). Cellulose crystallinity index: Measurement techniques and their impact on interpreting cellulase performance. *Biotechnology for Biofuels*, *3*, 1–10.

Petersson, L., Kvien, I., & Oksman, K. (2007). Structure and thermal properties of poly(lactic acid)/cellulose whiskers nanocomposite materials. *Composites Science and Technology*, *67*, 2535–2544.

Regourd, J., Ali, A. A.-S., & Thompson, A. (2007). Synthesis and anti-cancer activity of C-ring-functionalized prodigiosin analogues. *Journal of Medicinal Chemistry*, *50*, 1528–1536.

Samir, M. A. S. A., Alloin, F., & Dufresne, A. (2005). Review of recent research into cellulosic whiskers, their properties and their application in nanocomposite field. *Biomacromolecules*, *6*, 612–626.

Sebti, I., Chollet, E., Degraeve, P., Noel, C., & Peyrol, E. (2007). Water sensitivity, antimicrobial, and physicochemical analyses of edible films based on HPMC and/or chitosan. *Journal of Agricultural and Food Chemistry*, *55*, 693–699.

Siqueira, G., Bras, J., & Dufresne, A. (2009). Cellulose whiskers versus microfibrils: Influence of the nature of the nanoparticle and its surface functionalization on the thermal and mechanical properties of nanocomposites. *Biomacromolecules*, *10*, 425–432.

Siqueira, G., Bras, J., & Dufresne, A. (2010). New process of chemical grafting of cellulose nanoparticles with a long chain isocyanate. *Langmuir*, *26*, 402–411.

Thielemans, W., Belgacem, M. N., & Dufresne, A. (2006). Starch nanocrystals with large chain surface modifications. *Langmuir*, *22*, 4804–4810.

Wang, J., Wang, Z., Li, J., Wang, B., Liu, J., Chen, P., et al. (2012). Chitin nanocrystals grafted with poly(3-hydroxybutyrate-co-3-hydroxyvalerate) and their effects on thermal behavior of PHBV. *Carbohydrate Polymers*, *87*, 784–789.

Welsh, E. R., & Price, R. R. (2003). Chitosan cross-linking with a water-soluble, blocked diisocyanate. 2. Solvates and hydrogels. *Biomacromolecules*, *4*, 1357–1361.

Welsh, E. R., Schauer, C. L., Qadri, S. B., & Price, R. R. (2002). Chitosan cross-linking with a water-soluble, blocked diisocyinate. 1. Solid state. *Biomacromolecules*, *3*, 1370–1374.

Yu, J., Ai, F., Dufresne, A., Gao, S., Huang, J., & Chang, P. R. (2008). Structure and mechanical properties of poly(lactic acid) filled with (starch nanocrystal)-graft-poly(epsilon-caprolactone). *Macromolecular Materials and Engineering*, *293*, 763–770.